A Robustly Optimized Level Set Method for Accurate Cardiac Image Segmentation

Dr. Samad Wali

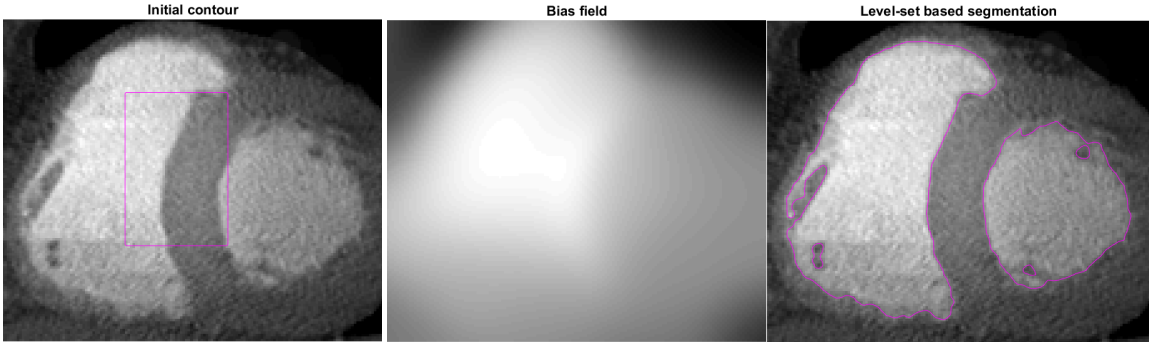
Faculty Member: General Education Centre,
Quanzhou University of Information Engineering
Fujian, China

October 30, 2026

Outline

1. Motivation for proposed work
2. Basic notations, level set methods, ADMM
3. Image restoration model (ROF, 1992) as an example
4. Image segmentation model as an example
5. Applications in cardiac medical image segmentation
6. Limitations
7. Future work

Motivation for Proposed Work



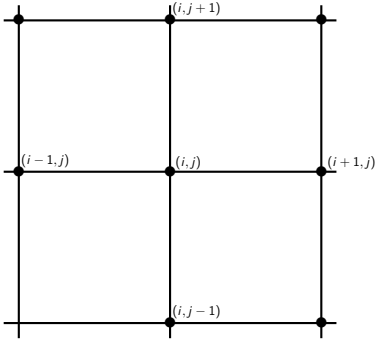
(a) Observed cardiac image[1]; $I(x) = b(x)C_k + \eta(x)$ (b) Bias field $b(x)$ estimation (c) Segmentation; $\phi^* = S_{ls}(I(x))$

Figure represents Results for CT heart image with bias field and noise via level set based segmentation.[2]

[1] Radiopaedia: https://radiopaedia.org/articles/cardiac-ct-1

[2] Samad Wali, et al., Signal Processing, 2023.

Basic Notation



We represent a grayscale image as an $M * N$ matrix. The discrete gradient operator is given by

$$(\nabla u)_{i,j} = ((D_x^+ u)_{i,j}, (D_y^+ u)_{i,j})$$

$$(D_x^+ u)_{i,j} = \begin{cases} u_{i+1,j} - u_{i,j}, & 1 \leq i < M, \\ u_{1,j} - u_{M,j}, & i = M, \end{cases}$$

Basic Notation

Level Set Representation in Image Segmentation

Key Idea

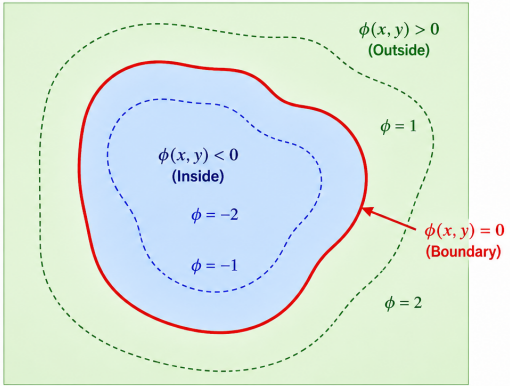
- A contour (boundary) is represented implicitly using a function $\phi(x, y)$, called the level set function.

Mathematical Interpretation

- The contour (object boundary) is defined by the zero level set:

$$\phi(x, y) = 0$$

- Region classification:
  - Inside the object : $\phi(x, y) < 0$
  - On the boundary : $\phi(x, y) = 0$
  - Outside the object : $\phi(x, y) > 0$



Summary

- Inside the object: $\phi(x, y) < 0$ (e.g., $\phi = -1, -2, \ldots$)
- On the boundary: $\phi(x, y) = 0$
- Outside the object: $\phi(x, y) > 0$ (e.g., $\phi = 1, 2, \ldots$)

Variational Model (classical inverse problem)

1. ROF Model [3]

$$\min_u TV(u) + \frac{\alpha}{2}\|I - u\|_2^2$$

where

$$TV(u) = \sum_{i,j} |(\nabla u)_{i,j}|$$

Here gradient decent method is bad due to its slow convergence..

[3] Rudin, Leonid I., Stanley Osher, and Emad Fatemi. "Nonlinear total variation based noise removal algorithms." Physica D: nonlinear phenomena, 1992.

Alternating Direction Method of Multipliers (ADMM); Introduction and Motivation

- **Robust method for optimization**
  Machine learning
  Image processing and engineering
  Statistics with huge data set
  Dynamic optimization on large-scale network
- **History**
  In 1970s [4]this method was developed with root in 1950s.
- **Related Methods**
  Split Bregman iteration scheme [5]
  Operator splitting methods [6] Proximal point algorithm (Rockafellar 1976)

[4]D. Gabay and B. Mercier "A dual algorithm for the solution of nonlinear variational problems via finite element approximation", 1976

[5]Donald K. Art of Computer Programming[M]. 1973.

[6]Douglas, Peaceman, Rachford, Lions, Mercier, ...1950s, 1979)

ADMM; General Formulation

Alternating direction method of multipliers or ADMM: combines the best of both methods (gradient decent and augmented Lagrangian method). Consider a problem of the form:

$$\min_{u,v} I(u) + g(v) \quad \text{subject to} \quad Au + Bv = c$$

We define augmented Lagrangian, for a parameter $\gamma > 0$

$$\mathcal{L}_\gamma(u, v; \lambda) = I(u) + g(v) + \lambda^T(Au + Bv - c) + \frac{\gamma}{2}\|Au + Bv - c\|_2^2$$

We repeat, for $k = 1, 2, 3, ...$

$$u^k = \arg\min_u \mathcal{L}_\gamma(u, v^{k-1}; \lambda^{k-1})$$

$$v^k = \arg\min_v \mathcal{L}_\gamma(u^k, v; \lambda^{k-1})$$

$$\lambda^k = \lambda^{k-1} + \gamma(Au^k + Bv^k - c)$$

Image Restoration Model (ROF, 1992) as an Example

Recall the TV problem or ROF model: The constrained problem:

$$\begin{aligned} &\min_{u,\mathbf{p}} \|\mathbf{p}\|_1 + \frac{\alpha}{2}\|I-u\|_2^2, \\ &\text{s.t.} \quad \mathbf{p} = \nabla u. \end{aligned} \tag{1}$$

The augmented Lagrangian for constraint problem (1) can be obtained as:

$$\mathcal{L}(u,\mathbf{p};\lambda) = \|\mathbf{p}\|_1 + \frac{\alpha}{2}\|I-u\|_2^2 + \langle \lambda, \mathbf{p}-\nabla u\rangle + \frac{\gamma}{2}\|\mathbf{p}-\nabla u\|_2^2. \tag{2}$$

ADMM steps [7]: for $k = 1, 2, 3, ...$

$$u^k = \mathcal{F}^{-1}\Big(\frac{\alpha\mathcal{F}(f) - \mathcal{F}(div)\mathcal{F}(\lambda^{k-1}+\gamma\mathbf{p}^{k-1})}{\alpha - \gamma\mathcal{F}(\Delta)}\Big),$$

$$\mathbf{p}^k = \begin{cases} \Big(1 - \frac{1}{\gamma}\frac{1}{|w_{i,j}|}\Big)w_{i,j} & \text{if } |w_{i,j}| > \frac{1}{\gamma}, \\ 0 & \text{otherwise,} \end{cases} \quad \text{where} \quad w_{i,j} = \nabla u^k - \frac{\lambda^{k-1}}{\gamma}$$

$$\lambda^k = \lambda^{k-1} + \gamma(\mathbf{p}^k - \nabla u^k).$$

[7] Wali, Samad, et al. "A boosting procedure for variational-based image restoration." Numerical Mathematics: Theory, Methods and Applications, 2018

Image Segmentation Model as an Example

Recall the DRLSE model: The constrained problem:

$$\min_{\phi,\varphi,u,q,p} \alpha \int_\Omega g|q| + \beta \int_\Omega gu + \frac{\mu}{2} \int_\Omega (|p| - 1)^2 \tag{3}$$

subject to the following constraints: $u = H(\varphi), \varphi = \phi, q = \nabla u, p = \nabla \phi$. The augmented Lagrangian energy is:

$$\begin{aligned} L(\phi, \varphi, u, q, p; \Lambda) = \alpha \int_\Omega g|q| + \beta \int_\Omega gu + \frac{\mu}{2} \int_\Omega (|p| - 1)^2 \\ + (\lambda_\varphi, \varphi - \phi) + \frac{r_\varphi}{2}(\varphi - \phi)^2 + (\lambda_u, u - H(\varphi)) + \frac{r_u}{2}(u - H(\varphi))^2 + \\ (\lambda_q, q - \nabla u) + \frac{r_q}{2}(q - u)^2 + (\lambda_p, p - \nabla \phi) + \frac{r_p}{2}(p - \nabla \phi)^2. \end{aligned} \tag{4}$$

Where $\Lambda = (\lambda_\varphi, \lambda_u, \lambda_q, \lambda_p)$ are the Lagrangian multipliers and r_φ, r_u, r_q, r_p are positive constants. Then the ADMM for solving (4) can be described in further ADMM Algorithm:

Overview of Classical Level Set with Bias Field Estimation

Consider the observed image $I(x)$ is assumed to satisfy the relation:

$$I(x) = b(x)C_k + \eta(x), \quad x \in \Omega_k, \quad k = 1, 2, \tag{5}$$

where $b(x)$ is the smoothly varying bias field, C_k represents the mean intensity of the k-th region, Ω_k is the corresponding segmented region, and $\eta(x)$ denotes additive noise.
The segmentation task is formulated as an energy minimization problem:

$$E(\phi, b, C) = \underbrace{\sum_k \int_\Omega M_k(x) \left(I(x) - b(x)C_k\right)^2 dx}_{\text{data fidelity term}} + \underbrace{\nu \int_\Omega \delta_\epsilon(\phi)|\nabla\phi| dx}_{\text{length regularization}} + \underbrace{\mu \int_\Omega \frac{1}{2}\left(|\nabla\phi| - 1\right)^2 dx}_{\text{distance regularization}}, \tag{6}$$

where ϕ is the level set function, $M_k(x)$ are membership functions obtained via a smoothed Heaviside function $H_\epsilon(\phi)$, $\delta_\epsilon(\phi)$ is the regularized Dirac delta function, and ν, μ are weighting coefficients controlling the smoothness and regularity of the contour.

GD Method[8]

In practice, the level set function ϕ is iteratively updated by gradient descent:

$$\phi^{n+1} = \phi^n + \Delta t \left(-\delta_\epsilon(\phi^n)(e_1 - e_2) + \mu(4\nabla^2\phi^n - K) + \nu\delta_\epsilon(\phi^n)K\right), \tag{7}$$

where $e_k = KONE \cdot I^2 - 2C_k K_b \cdot I + C_k^2 K_b^2$, K is curvature, and K_b denotes the Gaussian kernel applied to the bias field. The constants C_k and bias field $b(x)$ are updated in closed form:

$$C_k = \frac{\sum_x K_b \cdot b \cdot I \cdot M_k}{\sum_x K_b \cdot b^2 \cdot M_k}, \tag{8}$$

$$b = \frac{\sum_k K_b \cdot (C_k M_k) \cdot I}{\sum_k K_b \cdot C_k^2 M_k}. \tag{9}$$

[8] Li, Chunming, et al. "A level set method for image segmentation in the presence of intensity inhomogeneities with application to MRI." IEEE transactions on image processing. 2011

ADMM formulation

To improve convergence and robustness, we reformulate the LS–BFE problem using the "Alternating Direction Method of Multipliers (ADMM)". The segmentation problem is split into multiple subproblems by introducing auxiliary variables v, φ, and (q_x, q_y), which decouple the nonconvex terms in the energy functional. The augmented Lagrangian is written as:

$$\begin{aligned}\mathcal{L}(\phi, v, \varphi, q_x, q_y, \lambda_u, \lambda_q, \lambda_\varphi, \lambda_p) = &\sum_{k=1}^{2} \int_\Omega M_k(x) \left(I(x) - b(x) C_k\right)^2 dx \\ &+ \frac{r_u}{2} \|v - H_\epsilon(\varphi)\|_2^2 + \frac{r_q}{2} \|q_x - F_x(v)\|_2^2 + \frac{r_q}{2} \|q_y - F_y(v)\|_2^2 \\ &+ \frac{r_\varphi}{2} \|\varphi - \phi\|_2^2 + \frac{r_p}{2} \|p - \nabla\phi\|_2^2 \\ &+ \text{Lagrange multipliers terms.} \end{aligned} \tag{10}$$

Subproblem Updates

1. v-subproblem (Heaviside consistency)

$$v^{n+1} = \arg\min_{v} \frac{r_u}{2}\|v - H_\epsilon(\varphi^n) + \lambda_u/r_u\|_2^2 + \frac{r_q}{2}\|\nabla v - q^n + \lambda_q/r_q\|_2^2. \tag{11}$$

This is solved efficiently in the Fourier domain using FFT-based inversion.

2. q-subproblem (gradient shrinkage)

$$(q_x^{n+1}, q_y^{n+1}) = \arg\min_{q_x, q_y} \nu\|q\|_1 + \frac{r_q}{2}\|q - \nabla v^{n+1} + \lambda_q/r_q\|_2^2, \tag{12}$$

where the soft-thresholding (shrinkage) operator ensures edge-preserving regularization.

3. φ-subproblem (phase stabilization)

$$\varphi^{n+1} = \arg\min_{\varphi} \frac{r_\varphi}{2}\|\varphi - \phi^n + \lambda_\varphi/r_\varphi\|_2^2 + \frac{r_u}{2}\|H_\epsilon(\varphi) - v^{n+1} + \lambda_u/r_u\|_2^2, \tag{13}$$

solved using Newton iterations for accurate zero-crossing alignment.

Subproblem Updates

4. ϕ-subproblem (level set update)

$$\phi^{n+1} = \arg\min_{\phi} \frac{r_\varphi}{2}\|\phi - \varphi^{n+1} + \lambda_\varphi / r_\varphi\|_2^2 + \frac{r_p}{2}\|\nabla\phi - p^{n+1} + \lambda_p / r_p\|_2^2, \tag{14}$$

where the gradient term enforces distance regularization and smoothness. FFT is used for fast inversion. The bias field $b(x)$ and constants C_k are updated similarly to the classical model:

$$C_k = \frac{\sum_x K_b \cdot b \cdot I \cdot M_k}{\sum_x K_b \cdot b^2 \cdot M_k}, \tag{15}$$

$$b = \frac{\sum_k K_b \cdot (C_k M_k) \cdot I}{\sum_k K_b \cdot C_k^2 M_k}. \tag{16}$$

Test our proposed method



Synthetics images for testing and comparing our proposed method.

Test Our Proposed Method and Compare with EDRLSE [9], RESLS [10] and DRLSU-Net [11]

Table 1: Size, iterations, time in seconds, and dice of our proposed method versus EDRLSE [16], RESLS [17] and DRLSU-Net [18] on five test images.

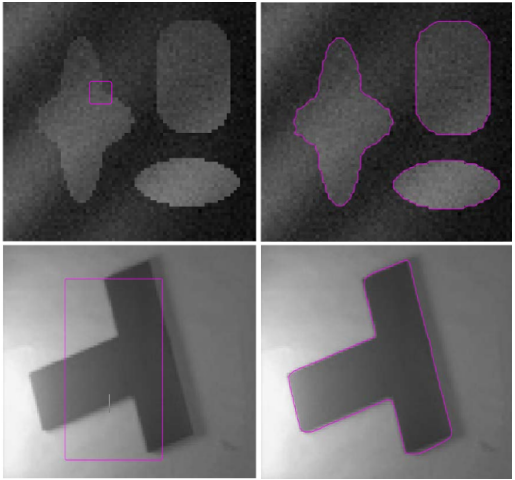
Image	Size	Iters	Time (sec)				Dice			
			EDRLSE	RESLS	DRLSU-Net	Ours	EDRLSE	RESLS	DRLSU-Net	Ours
Camel	346 × 346	100	5.0569	4.6640	2.0433	0.4567	0.7381	0.6443	0.8486	0.9119
Deer	691 × 550	110	11.8218	9.8620	3.6112	2.2567	0.6768	0.6959	0.7787	0.8335
Cup	356 × 315	150	6.1120	4.9951	2.1342	0.5360	0.6845	0.6911	0.7495	0.8053
Beetle	201 × 198	150	4.9022	3.5671	0.9292	0.3021	0.6910	0.6423	0.7345	0.8286
QR code	474 × 474	150	9.0910	7.2211	2.3442	1.6624	0.7134	0.6538	0.7884	0.8512

[9] Wali Samad et al. (2023). Level-set evolution for medical image segmentation with ADMM Signal Processing, 2023.

[10] Zhang, Wang at el., RESLS: Region and edge synergetic level set framework for image segmentation. IEEE Transactions on Image Processing, 2019.

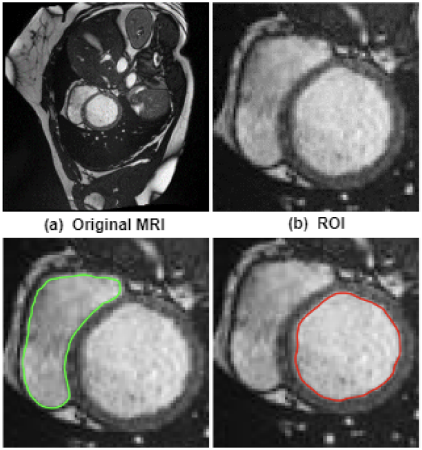
[11] Wang, Xie et al., DRLSU-Net: Level set with U-Net for medical image segmentation. Digital Signal Processing, 2025.

Natural Image Results



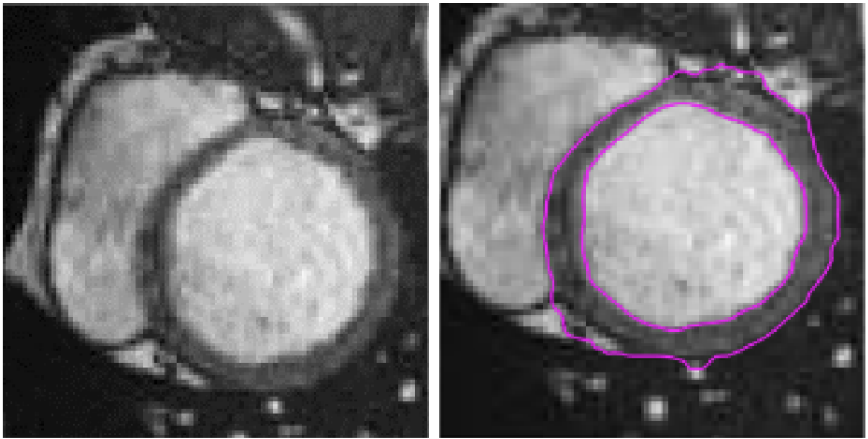
In this Fig., we present the segmentation results obtained on some natural images. We evaluate the effectiveness of the proposed method under degradations caused by different types of noise and blur effects. (Dice: 0.9826, Time: 0.04 Sec)

Medical Image Results (cardiac)



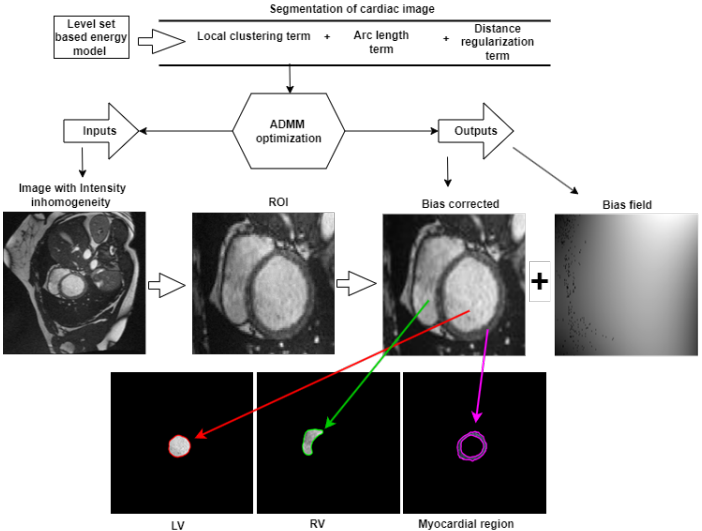
In this Fig, Short axis cine-MRI view of one representative patient: (a) Original MRI, (b) Region of interest (ROI) (c) Right ventricle region (d) Left ventricle region.

Medical Image Results (cardiac)



Clinical MR image showing the myocardial infarction area: (a) Original scanned image, (b) Segmented myocardial region.

Summary (graphical abstract)



Overview of the Proposed Framework. The diagram provides a schematic representation of the components.

Limitations

1. Dataset Generalization Constraints (one input one output)
2. Parameter Sensitivity (manually handle)

- eg: $\nu, \mu, r_u, r_q, r_p, r_\varphi$

3. Sensitivity to Initialization

- Although ADMM improves convergence behavior, the level set framework can still be sensitive to the initial contour placement.
- Poor initialization may lead to local minima, especially in low-contrast boundaries.

Ongoing Work

1. Integrate CNN-based feature extraction (e.g., U-Net encoder), ImagNet, and Segnet with level set evolution:
- Use deep features to guide contour evolution
- Improve robustness to complex textures and pathologies
2. Use ADMM for efficient error estimations in deep learning problems
3. Adaptive Parameter Learning via Optimization or AI Incorporate automatic parameter tuning:
- Bayesian optimization reinforcement learning
- meta-learning to eliminate manual intervention
4. Extension to 3D + Temporal Segmentation (4D Cardiac Data) Expand the method to:
- 3D volumetric segmentation
- time-resolved cardiac sequences (cine MRI)

References

[1] Wali, S., Li, C., Imran, M., Shakoor, A., Basit, A. (2023). Level-set evolution for medical image segmentation with alternating direction method of multipliers. Signal Processing, 211, 109105, 2023.

[2] Li, Chunming, et al. "A level set method for image segmentation in the presence of intensity inhomogeneities with application to MRI." IEEE transactions on image processing 20.7 (2011): 2007-2016.

[3] Zhang, W., Wang, X., You, W., Chen, J., Dai, P., Zhang, P.. RESLS: Region and edge synergetic level set framework for image segmentation. IEEE Transactions on Image Processing, 29, 57-71, 2019.

[4] Wang, X., Liu, J., Yang, R., Wu, Z., Sun, L., Zou, L. . DRLSU-Net: Level set with U-Net for medical image segmentation. Digital Signal Processing, 157, 104884, 2025.

[5] Olaf Ronneberger, Philipp Fischer, Thomas Brox "U-Net: Convolutional Networks for Biomedical Image Segmentation", MICCAI, 2015.

[6] Jia Deng, Wei Dong, Richard Socher, Li-Jia Li, Kai Li, Fei-Fei Li "ImageNet: A Large-Scale Hierarchical Image Database", CVPR, 2009.

[7] Vijay Badrinarayanan, Alex Kendall, Roberto Cipolla "SegNet: A Deep Convolutional Encoder-Decoder Architecture for Image Segmentation", IEEE TPAMI, 2017.

Thank You